

Thermally Cleavable Surfactants Based on Furan–Maleimide Diels–Alder Adducts

James R. McElhanon,[†] Thomas Zifer,[†] Steven R. Kline,[‡] David R. Wheeler,[§]
Douglas A. Loy,^{||} Gregory M. Jamison,[⊥] Timothy M. Long,[⊥]
Kamyar Rahimian,[⊥] and Blake A. Simmons^{*,†}

Materials Chemistry Department, Sandia National Laboratories, Livermore, California 94551, NIST Center for Neutron Research, National Institute of Standards and Technology, Gaithersburg, Maryland 20899, Micro-Total-Analytical Systems Department, Sandia National Laboratories, Albuquerque, New Mexico 87185, Polymers and Coatings Group, Los Alamos National Laboratory, Los Alamos, New Mexico 87545, and Chemical Synthesis and Nanomaterials Department, Sandia National Laboratories, Albuquerque, New Mexico 87185

Received November 29, 2004

Two new surfactant molecules are reported that contain thermally labile Diels–Alder adducts connecting the hydrophilic and hydrophobic sections of each molecule. The two surfactants possess identical hydrophobic dodecyl tail segments but have phenol and carboxylic acid hydrophilic headgroups, respectively. Deprotonation with potassium hydroxide affords the formation of water-soluble surfactants. Room temperature aqueous solutions of both surfactants exhibit classical surface-active agent behavior similar to common analogous alkylaryl surfactant molecules. Critical micelle concentrations have been determined for each surfactant through dynamic surface tension and dye solubilization techniques. Small-angle neutron scattering measurements of the aqueous surfactant solutions indicate the presence of spherical micelles with radii of 16.5 Å for the carboxylate and 18.8 Å for the phenolate. When these surfactants are exposed to elevated temperatures (>50 °C), the retro Diels–Alder reaction occurs, yielding hydrophilic and hydrophobic fragments. Aqueous solutions of each surfactant subsequently exhibit a loss of all surface-active behavior and the micellar aggregates are no longer detectable.

Introduction

Over the past decade, the development of cleavable surfactants has been a growing field in surfactant science.¹ As the name implies, cleavable surfactants are molecules that undergo a chemical or physical change of the parent molecular structure resulting in a change and/or loss of surface-active behavior. Hence, the production of commercially available cleavable surfactants would find utility in industrial practices where foaming or persistent surface-active properties must be diminished after their initial use, in green chemistry where biodegradability is of primary concern, and in biomedical drug delivery where surfactants could be removed through biological mechanisms.¹

Surfactant removal becomes increasingly significant in the synthesis of extended mesoporous and nanosized structures such as semiconductor nanocrystals,² ceramics,³ polymers,⁴ and polymer–ceramic composites.⁵ Current techniques of surfactant removal are typically some combination of centrifugation, calcination, and solvent

washing steps that can adversely affect and/or completely destroy the desired extended architecture and functionality of the synthesized material.⁶ Incorporation of a cleavable linkage into surfactant molecules could solve this problem by allowing the removal of the surfactant templates through the thermally triggered formation of small, easily removed fragments.

Several examples of cleavable surfactants have been previously reported based on functional groups that are susceptible to alkaline or acid hydrolysis. The surfactants operate within defined pH ranges and are removed from the system by adding an appropriate amount of acid or base. Acid-labile surfactants include cationic surfactants with cyclic acetals such as cationic surfactants derived from bromopropionaldehyde,⁷ alkylglucosides,⁸ ortho esters,⁹ and both cyclic¹⁰ and noncyclic ketals.¹¹ Alkaline-labile surfactants include surfactants that contain cleavable ester moieties such as choline esters,¹² esters of quaternized amidoamines¹³ and ethanolamines,¹⁴ as well

* Corresponding author. E-mail: basimmo@sandia.gov. Phone: 925-294-2288. Fax: 925-294-3410.

[†] Materials Chemistry Department, Sandia National Laboratories.

[‡] National Institute of Standards and Technology.

[§] Micro-Total-Analytical Systems Department, Sandia National Laboratories.

^{||} Los Alamos National Laboratory.

[⊥] Chemical Synthesis and Nanomaterials Department, Sandia National Laboratories.

(1) Holmberg, K. *Novel Surfactants. Preparation, Applications, and Biodegradability*; Marcel Dekker, Inc.: New York, 1998; pp 334–340.

(2) Simmons, B.; Irvin, G.; Agawam, V.; Bose, A.; John, V.; McPherson, G.; Basra, N. *Langmuir* **2002**, *18* (3), 624–632.

(3) Sims, S. D.; Walsh, D.; Mann, S. *Adv. Mater.* **1998**, *10* (1), 151–154.

(4) Irvin, G.; Bannerjee, S.; Premachandran, R.; Simmons, B.; Li, S.; John, V.; McPherson, G.; Akkara, J.; Kaplan, D.; Zhou, W. *Reactions and Synthesis in Surfactant Systems*; Surfactant Science Series 100; Marcel Dekker: New York, 2001; pp 515–524.

(5) Kimura, T.; Suzuki, M.; Tomura, S.; Oda, K. *Chem. Lett.* **2003**, *2*, 188–192.

(6) Li, S.; John, V. T.; Rachakonda, S.; Irvin, G.; McPherson, G.; O'Connor, C. J. *J. Appl. Phys.* **1999**, *85*, 5178–5180.

(7) Wang, G.-W.; Yuan, X.-Y.; Liu, Y.-C.; Lei, X.-G.; Guo, Q.-X. *J. Am. Oil Chem. Soc.* **1995**, *72*, 83–87.

(8) Balzer, D. *Spec. Surfactants* **1997**, 169–207.

(9) Eliason, R.; Kreevoy, M. M. *J. Am. Chem. Soc.* **1978**, *100*, 7037–7041.

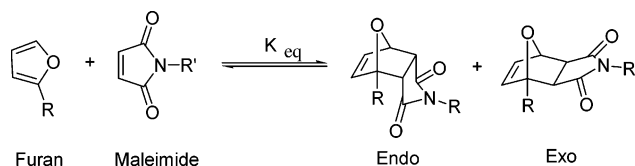
(10) Jaeger, D. A.; Sayed, Y. M. *J. Org. Chem.* **1993**, *58*, 2619–2627.

(11) Ono, D.; Masuyama, A.; Okahara, M. *J. Org. Chem.* **1990**, *55*, 4461–4464.

(12) Lindstedt, M.; Allenmark, S.; Thompson, R. A.; Edebo, L. *Antimicrob. Agents Chemother.* **1990**, *34*, 1949–1954.

(13) Lagerman, R.; Clancy, S.; Tanner, D.; Johnston, N.; Callian, B.; Friedli, F. J. *J. Am. Oil Chem. Soc.* **1994**, *71*, 97–100.

Scheme 1. Furan–Maleimide Diels–Alder Adduct Formation and Dissociation



as esters derived from naturally occurring sugars (i.e., glucose, sucrose, and sorbitol) combined with fatty acids.¹⁵ One disadvantage of these hydrolyzable surfactants is the requisite addition of acid or base to degrade the surfactant. Other labile elements that have been incorporated into surfactants include UV sensitive components, such as alkylaryl ketone sulfonates¹⁶ and diazosulfonates¹⁷ that degrade upon irradiation. Thermally labile surfactants include amine oxide surfactants which decompose at high temperatures.¹⁸ In addition, there are some reports of photoresponsive surfactants that dimerize or undergo conformational isomerization when irradiated with UV light, resulting in changes in surface-active behavior without surfactant degradation.¹⁹

We report here the synthesis and characterization of two new surfactants that incorporate a thermally cleavable Diels–Alder adduct as the chemical weak link within the surfactant molecular structure. The Diels–Alder reaction involves a [4 + 2] cycloaddition reaction between a diene and a dienophile.²⁰ We have utilized the reversible Diels–Alder (DA) reaction between functionalized furans and maleimides as the basis for our thermally cleavable materials (Scheme 1).²¹ Previously, we reported the integration of furan–maleimide DA adducts into molecules to produce thermally responsive encapsulants,²² foams,²³ and adhesives,²⁴ as well as dendrons and dendrimers which reversibly self-assemble.²⁵ Recent reports exist which incorporate similar thermally reversible DA adducts into responsive polymers.²⁶ The process of adduct formation typically occurs at moderate temperatures (25–60 °C), whereas dissociation occurs at elevated temperatures (>60 °C), as shown in Scheme 1. Surfactant molecules that contain cleavable furan–maleimide DA adducts (Scheme 2) are, therefore, attractive candidates

as surface-active materials for processes that require surfactant “deactivation” or removal using a noninvasive thermal trigger. Previous work in the area of Diels–Alder surfactants has concentrated on reacting 1,3-diene detergents with hydrophilic dienophiles to aid in the solubilization of enzymes.²⁷ In addition, Diels–Alder reactions between different surfactants have been shown to provide a high degree of regioselectivity for specific reaction chemistries.²⁸ This work is, to the best of our knowledge, the first report of incorporating thermally labile DA adducts within surfactant structures themselves.

Experimental Section

Materials and Methods. All NMR spectra were measured at 500 MHz ¹H and 125 MHz ¹³C in CDCl₃, DMSO-*d*₆, or D₂O unless otherwise specified. Elemental analyses were performed by Gailbraith Laboratories of Knoxville, TN. Acetone, diethyl ether, chloroform, petroleum ether, and ethyl acetate were obtained from Aldrich Chemical Co., Inc. and used as received. Reagent grade chemicals (Orange OT, Sudan III, 1.0 N potassium hydroxide (KOH) aqueous solution standard, and triethylamine) were obtained from Aldrich Chemical Co., Inc. Deuterium oxide (D₂O) and potassium deuterioxide (30% in D₂O) were obtained from Acros Organics. *N*-(4-Hydroxyphenyl)maleimide, *N*-(4-carboxyphenyl)maleimide, and 2-*N*-dodecylfuran were prepared according to the literature.^{29,30} Flash chromatography was performed by the method of Still et al.³¹ using silica gel (200–400 mesh, 60 Å). Thin-layer chromatography (TLC) was performed on precoated TLC plates (silica gel, 250 μm (Aldrich)). All other reagents were purchased from commercial suppliers and used as received. Doubly filtered deionized water with a resistance of 18.2 MΩ was used for all experiments unless otherwise noted.

Preparation of Surfactants. *exo*-4-Dodecyl-7-oxabicyclo-[2.2.1]hept-5-ene-2,3-dicarboxy-*N*-(4-hydroxyphenyl)imide (**4**). To a solution of *N*-(4-hydroxyphenyl)maleimide (**1**) (3.15 g, 16.6 mmol) in acetone (40 mL) was added alkyl furan (**3**) (5.62 g, 23.8 mmol). The reaction was allowed to stir at 55 °C until TLC (SiO₂, 1:1 petroleum ether–ethyl acetate) showed consumption of the starting material. The reaction was then concentrated to dryness and the residue purified by flash chromatography (SiO₂, 1:9 ethyl acetate–petroleum ether) to yield **4** (6.80 g, 96%) as a colorless solid. ¹H NMR (500 MHz, CDCl₃, δ): 7.07 (d, *J* = 9.0 Hz, 2H), 6.80 (d, *J* = 8.5 Hz, 2H), 6.52 (dd, *J* = 5.0, 2.0 Hz, 1H), 6.41 (d, *J* = 6 Hz, 1H), 5.32 (s (br), 1H), 5.29 (d, *J* = 1.5 Hz, 1H), 3.07 (d, *J* = 6.5 Hz, 1H), 2.87 (d, *J* = 6.5 Hz, 1H), 2.13–1.95 (m, 2H), 1.66–1.43 (m, 2H), 1.40–1.19 (m, 18H), 0.86 (t, *J* = 7.5 Hz, 3H). ¹³C (125 MHz, CDCl₃, δ): 176.20, 174.72, 156.24, 139.12, 136.91, 127.92, 123.87, 116.14, 92.30, 80.82, 50.45, 49.00, 31.88, 29.91, 29.71, 29.63, 29.60, 29.52, 29.48, 29.31, 25.32, 22.65, 14.08. Anal. Calcd for C₂₆H₃₅NO₄: C, 73.38; H, 8.29; N, 3.29. Found: C, 73.13; H, 8.49; N, 3.26.

exo-4-Dodecyl-7-oxabicyclo[2.2.1]hept-5-ene-2,3-dicarboxy-*N*-(4-carboxyphenyl)imide (**5**). *N*-(4-Carboxyphenyl)maleimide (**2**) (3.68 g, 16.9 mmol) was added to a solution of alkyl furan (**3**) (5.72 g, 24.2 mmol) and acetone (30 mL) and was heated to 55 °C. The reaction was left at 60 °C until TLC (SiO₂, 1:1 acetone–petroleum ether) indicated consumption of the starting material. The reaction was then concentrated to dryness, and the residue was purified by flash chromatography (SiO₂, 1:4 acetone–chloroform) and subsequently recrystallized (chloroform–petroleum ether) to yield **5** (5.37 g, 70%) as a colorless solid. ¹H NMR (500 MHz, CDCl₃, δ): 8.19 (d, *J* = 8.5 Hz, 2H), 7.44

(14) Swartley, D. M.; Trinh, T.; Wahl, E. H.; Huysse, G. M. U.S. Patent 5399272 A 950321, 1995.

(15) Ducret, A.; Giroux, A.; Trani, M.; Lortie, R. *J. Am. Oil Chem. Soc.* **1996**, *73*, 109–113.

(16) Epstein, W. W.; Jones, D. S.; Bruenger, E.; Rilling, H. C. *Anal. Biochem.* **1982**, *119*, 304–312.

(17) Nuyken, O.; Meindl, K.; Wokaun, A.; Mezger, T. *J. Photochem. Photobiol., A* **1995**, *85*, 291–298.

(18) Hayashi, Y.; Shirai, F.; Shimizu, T.; Nagano, Y.; Teramura, K. *J. Am. Oil Chem. Soc.* **1985**, *62*, 555–557.

(19) (a) Eastoe, J.; Dominguez, M. S.; Wyatt, P.; Beeby, A.; Heenan, R. K. *Langmuir* **2002**, *18*, 7837–7844. (b) Kang, H. C.; Lee, B. M.; Yoon, M. *J. Colloid Interface Sci.* **2000**, *231*, 255–264. (c) Evans, S. D.; Johnson, S. R.; Ringsdorf, H.; Williams, L. M.; Wolf, H. *Langmuir* **1998**, *14*, 6436–6440.

(20) Kwart, H.; King, K. *Chem. Rev.* **1968**, *68*, 415–447.

(21) Goussé, C.; Gandini, A.; Hodge, P. *Macromolecules* **1998**, *31*, 314–321.

(22) (a) Small, J.; Loy, D. A.; Wheeler, D. R.; McElhanon, J. R.; Saunders, R. S. U.S. Patent 6271335 B1, 2001. (b) Loy, D. A.; Wheeler, D. R.; McElhanon, J. R.; Durbin-Voss, M. L. U.S. Patent 6403753 B1, 2002.

(23) McElhanon, J. R.; Russick, E. M.; Wheeler, D. R.; Loy, D. A.; Aubert, J. H. *J. Appl. Polym. Sci.* **2002**, *85*, 1496–1502.

(24) (a) Aubert, J. H. *J. Adhes.* **2003**, *79*, 609–616. (b) Aubert, J. H. U.S. Patent 2003116272 A1, 2003.

(25) McElhanon, J. R.; Wheeler, D. R. *Org. Lett.* **2001**, *3* (17), 2681–2683.

(26) (a) Chen, X.; Wudl, F.; Mal, A. K.; Shen, H.; Nutt, S. R. *Macromolecules* **2003**, *36*, 1802–1807. (b) Chen, X.; Dam, M. A.; Ono, K.; Mal, A.; Shen, H.; Nutt, S. R.; Sheran, K.; Wudl, F. *Science* **2002**, *295*, 1698–1702.

(27) Keana, J. F.; Guzikowski, A. P.; Morat, C.; Volwerk, J. J. *J. Org. Chem.* **1983**, *48*, 2661–2666.

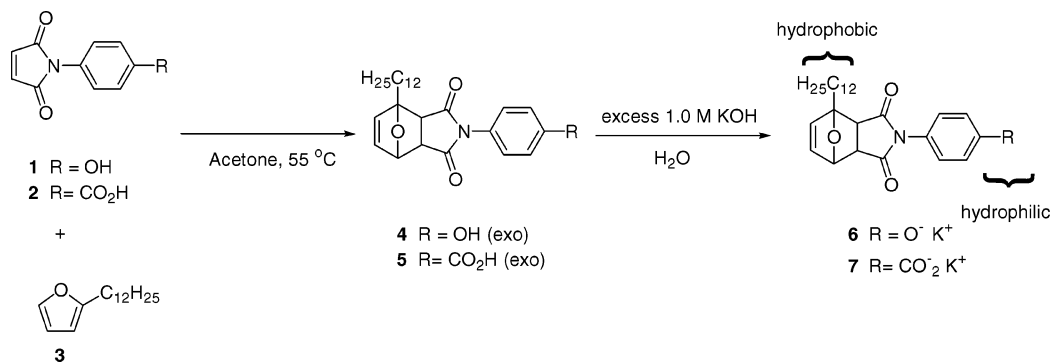
(28) Su, D.; Jaeger, D. A. *Tetrahedron Lett.* **1999**, *40*, 7871–7874.

(29) For the preparation of maleimides, see: Park, J. O.; Jang, S. H. *J. Polym. Sci., Polym. Chem. Ed.* **1992**, *30*, 723–729.

(30) For the preparation of 2-alkylfurans, see: Piancatelli, G.; Scettri, A.; D'Auria, M. *Tetrahedron* **1980**, *36*, 661–663.

(31) Still, W. C.; Kahn, M.; Mitra, A. *J. Org. Chem.* **1978**, *43*, 2923–2925.

Scheme 2. Synthesis Route to Surfactants with Diels–Alder Adducts Located between Hydrophilic and Hydrophobic Segments



(d, $J = 9.0$ Hz, 2H), 6.55 (dd, $J = 5.5, 1.5$ Hz, 1H), 6.43 (d, $J = 6.0$ Hz, 1H), 5.32 (d, $J = 1.5$ Hz, 1H), 3.12 (d, $J = 6.5$ Hz, 1H), 2.92 (d, $J = 6.5$ Hz, 1H), 2.14–1.96 (m, 2H), 1.66–1.44 (m, 2H), 1.41–1.26 (m, 18H), 0.86 (t, $J = 7.0$ Hz, 3H). ¹³C (125 MHz, CDCl₃, δ): 174.88, 173.48, 170.66, 139.24, 137.02, 136.47, 131.00, 129.08, 126.39, 92.48, 81.02, 50.59, 49.17, 31.90, 29.93, 29.72, 29.65, 29.62, 29.53, 29.48, 29.33, 25.34, 22.67, 14.10. Anal. Calcd for C₂₇H₃₅NO₅: C, 71.50; H, 7.78; N, 3.09. Found: C, 71.60; H, 7.88; N, 3.06.

Aqueous Surfactant Sample Preparation. Aqueous solutions were prepared by adding the appropriate amounts of **4** or **5** into deionized water. All samples were contained in 20 mL glass scintillation vials and capped with Teflon sealed screw caps. Because the protonated forms of **4** and **5** were only sparingly soluble in water, their conjugate bases (**6** and **7**) were prepared by the addition of potassium hydroxide. It was necessary to add excess amounts of potassium hydroxide to the solutions in order to obtain completely clear and isotropic surfactant solutions. The amount of excess potassium hydroxide required to completely solubilize the surfactant was found to be dependent on the surfactant headgroup present, with minimum molar ratios of 1.7:1 KOH–surfactant for the carboxylate surfactant (**7**) and 10:1 KOH–surfactant for the phenolate surfactant (**6**). The final pH of these aqueous solutions was 8.9 and 10.8 for the carboxylic and phenolic salts, respectively. We prepared aqueous solutions of the precursors **1**, **2**, and **3** in a similar fashion. For the solutions containing the headgroups **1** and **2**, these molecules were deprotonated by adding the same molar ratio of KOH (10:1 and 2:1, respectively) required to fully solubilize their respective surfactants **6** and **7** before conducting the surface tension measurements. This was done to establish the representative solution conditions that are expected to be present after surfactant degradation. Solutions of the alkyl furan (**3**) were observed to be oil and water mixtures irrespective of the amount of KOH added.

Dynamic Surface Tension. Surface tension measurements were conducted using a SensaDyne (Mesa, AZ) QC3000 dynamic surface tensiometer that utilizes the maximum bubble pressure method. The fundamental operating principles and theoretical considerations of this method are explained in detail elsewhere,³² and a brief summary only is given here. Two glass probes with different orifice diameters (0.5 and 4.0 mm) were submerged in an aqueous surfactant solution, and nitrogen was bubbled through the samples. Dry nitrogen was used as the bubble source gas and was delivered to the instrument at 50 psi. The instrument was operated at a bubble frequency of 2 Hz to approximate equilibrium surface tension values for each sample.³² The differential pressure signal generated by bubble formation is related to the interfacial surface tension of the liquid and gas. Surface tension calibration was carried out by measuring the surface tension of deionized water and ethanol and comparing it to known literature values. Solution temperature was monitored with a calibrated thermistor (± 0.1 °C) attached to the orifice probes. Instrumental calibration was conducted for every change

in experimental conditions and after prolonged periods of instrumental quiescence. All experiments were conducted at 26.0 ± 0.2 °C unless otherwise noted. Time averaging of the data produced values that differed by less than 0.2 mN/m from the mean. To determine the effect of temperature on surface tension as a measurement of surfactant degradation, the samples were heated at 95 °C for specified time intervals, allowed to cool to room temperature, and then analyzed. To determine the possible surface tension values expected of the surfactant solutions after cleaving, we measured the dynamic surface tension values for 20 mM solutions of the surfactant precursor molecules **1**, **2**, and **3**. Data were recorded for all experiments via a computer interface using the SensaDyne QC3000 version 5.3 software.

Dye Solubilization. To investigate the enhanced solubility of a water-insoluble dye in the presence of micelles, excess amounts (0.02 g/10 mL of aqueous sample) of both Orange OT and Sudan III were added to separate concentration series of aqueous surfactant solutions and sonicated for 30 min in a water bath operated under ambient conditions. The solutions were then removed from the sonicator and allowed to settle under ambient conditions for 2 h. The solutions were filtered using 0.2 μ m PVDF syringe filters (Whatman) into 3.5 mL 1 cm path length quartz cuvettes (Starna Cells, Inc.). The amount of dye solubilized in each sample was measured by monitoring the absorbance wavelength of each with a Shimadzu (Pleasanton, CA) 2401-PC UV–vis dual beam spectrophotometer operating under ambient conditions with surfactant solutions at equal concentrations without dyes serving as the sample background. Due to sample limitations, only two samples of each surfactant were analyzed and the mean was reported. Thus, no statistical analysis of the data was performed and reported.

Small-Angle Neutron Scattering. Small-angle neutron scattering (SANS) experiments were performed at the NG7 beamline at the NIST Center for Neutron Research (NCNR) in Gaithersburg, MD. The measurements determined the absolute scattering intensity ($I(q)$) as a function of the wave vector (q) ($=[4\pi/\lambda] \sin[\theta/2]$, where λ is the incident neutron wavelength and θ the scattering angle). The q range for these experiments was set to cover the range 0.003–0.19 \AA^{-1} , the neutron wavelength was set at 10 \AA , and the sample-to-detector distance was set to 10 and 1.9 m in order to encompass the stated q range. Sample concentrations were held constant at 15 mM in D₂O, which served as the neutron scattering contrast element. The required molar amounts of KOH listed above were added to the samples to form the anionic surfactants **6** and **7**. Samples were placed in quartz cells with a path length of 1 or 2 mm. The SANS data obtained were fitted using software programs developed at NCNR, which allows for various models to be tested covering a wide range of micellar geometries (i.e., vesicles, spheres, cylinders, disks, prolates, etc.). Instrumental resolution is included in these model calculations. It was determined that the polydisperse hard sphere model and a power-law plus hard sphere model were the best possible model fits to the data obtained from **6** and **7**, respectively. To determine the effect of thermally induced cleavage on micellar stability, the samples were heated at 95 °C for 2 h, allowed to cool to room temperature, and then placed in the SANS beamline sample holder for analysis.

(32) (a) Manglik, R. M.; Wasekar, V. M.; Zhang, J. *Exp. Therm. Fluid Sci.* **2001**, *25*, 55–64. (b) Renouf, P.; Hebrault, D.; Desmurs, J.-R.; Mercier, J.-M.; Mioskowski, C.; Lebeau, L. *Chem. Phys. Lipids* **1999**, *99*, 21–32.

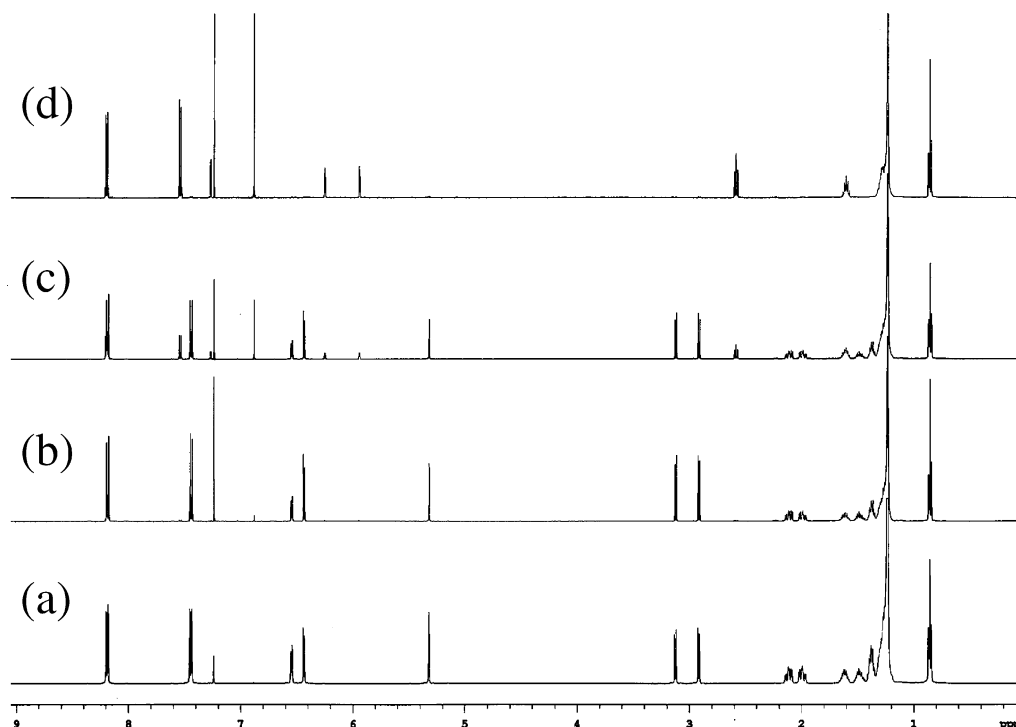


Figure 1. ^1H NMR spectra of **5** after solid state heating for 30 min at (a) 25 °C, (b) 105 °C, (c) 120 °C, and (d) 125 °C.

Results and Discussion

A. Synthesis of Diels–Alder Surfactants and Study of Thermal Lability by ^1H NMR. Neutral phenol (**4**) was prepared through the Diels–Alder (DA) addition of *N*-(4-hydroxyphenyl)maleimide (**1**) to 2-*n*-dodecyl furan (**3**) in acetone at 55 °C. Carboxylic acid (**5**) was prepared in a similar fashion through reaction of *N*-(4-carboxyphenyl)maleimide (**2**) with furan (**3**) under the same conditions (Scheme 2). We noted that the rate of reaction could be significantly accelerated through a series of solvent evaporation steps at elevated temperature, reducing the reaction time from weeks to days. Surfactant precursors **4** and **5** were isolated as colorless solids in 96 and 70% yields, respectively, after purification by flash chromatography on silica gel and recrystallization. Compounds **4** and **5** were characterized by ^1H and ^{13}C NMR spectroscopy and combustion analysis. The elevated temperature and solvent evaporation steps ensured complete conversion to the thermodynamically stable exo isomer for both **4** and **5**.²⁵ Water-soluble surfactants **6** and **7** were prepared *in situ* through deprotonation of **4** and **5** with excess KOH in water. Phenol (**4**) and carboxylic acid (**5**) required 10 and 1.7 equiv of KOH, respectively, to form completely soluble solutions of surfactants **6** and **7**. It is likely that the differences in headgroup polarity between **6** and **7** and potassium ion concentration are responsible for the excess KOH equivalents required to promote solubility of **6** and **7** in water.

The onset of the thermally reversible reactions of **4** and **5** in DMSO-*d*₆ solution was evaluated by ^1H NMR. Both **4** and **5** were thermally stable up to 50 °C at which point each compound began to undergo the retro DA reaction. Significant reversibility back to starting materials occurred at 60 °C for **4** (7% dissociation) and **5** (13% dissociation), as evidenced by the appearance of characteristic resonances for **1**, **2**, and **3** in the NMR spectra. For example, the singlets appearing at 7.07 ppm for **1** and 7.17 ppm for **2** corresponding to the two equivalent alkene protons in each were diagnostic in evaluating the onset

of the retro DA reaction for **4** and **5**, respectively. The solid state stability of **4** and **5** at elevated temperatures was also evaluated. Solid samples were incrementally heated, cooled to room temperature, and evaluated by NMR. Phenol (**4**) was stable with the DA adduct remaining intact up to 100 °C. Upon heating to 105 °C, the solid liquefied and ^1H NMR revealed >95% dissociation to the starting materials **1** and **3** (Scheme 2). Carboxylic acid (**5**) showed similar stability up to 105 °C with substantial conversion (>95%) to starting materials **2** and **3** at 125 °C (Figure 1).

The room temperature stability of **6** and **7** in water and their retro DA reactions in aqueous solutions at elevated temperatures were also investigated. ^1H NMR samples of surfactants **6** and **7** were prepared through treatment of **4** and **5** with appropriate amounts of KOD in D₂O. Phenolate (**6**) exhibited stability up to 55 °C at which point some small amount of degradation occurred, apparently not due to the retro DA reaction, as evidenced by the appearance of anomalous peaks in the ^1H NMR spectrum. Heating to 65 °C promoted **6** to undergo the retro DA reaction with substantial reversibility occurring by 75 °C, resulting in the formation of **3** and the potassium salt of **1**. Prolonged heating (3 h) at 95 °C converted the potassium salt of **1** to the corresponding ring-opened maleamic acid salt due to reaction with residual KOD. Surfactant **7** exhibited a similar trend with stability up to 50 °C at which point the retro DA reaction was activated with substantial fragmentation occurring at 60 °C. Furan (**3**) was observed in addition to the potassium salt of **2** upon heating at 95 °C in the presence of excess KOD for 3 h.

B. Critical Micelle Concentration Determination and Surface-Active Properties. Essential for characterizing a surfactant are to determine the extent to which it is a surface-active agent, to confirm the presence of micellar aggregates, and to determine the critical micelle concentration (cmc) above which these aggregates form. We have employed two traditional methods to achieve

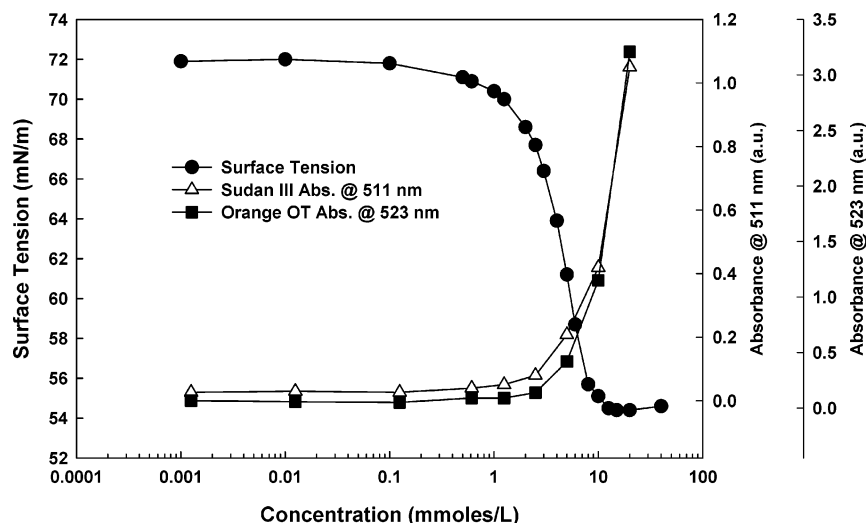


Figure 2. Semilog plot of the critical micelle concentration determination for the carboxylate surfactant (**7**) as determined by dynamic surface tension (operated in equilibrium mode) and dye solubilization measurements as a function of concentration at 26 °C.

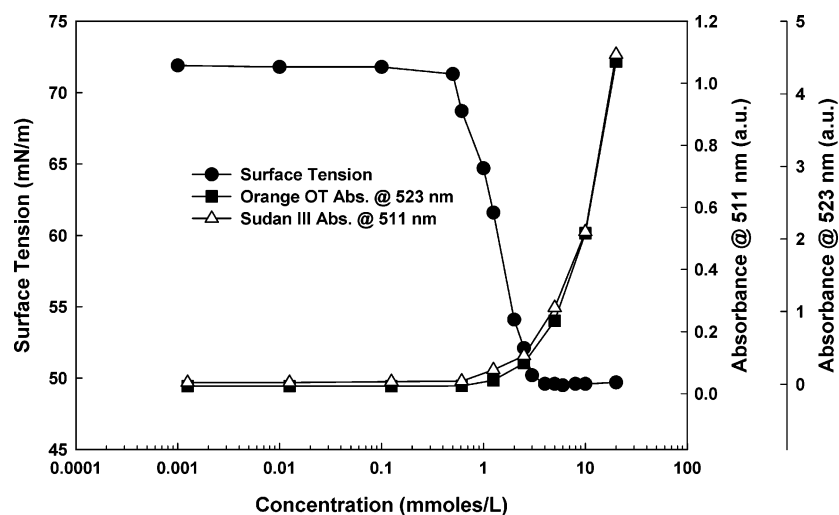


Figure 3. Semilog plot of the critical micelle concentration determination for the phenolate surfactant (**6**) as determined by dynamic surface tension (operated in equilibrium mode) and dye solubilization measurements as a function of concentration at 26 °C.

this surface tension and dye solubilization. The solubilization of a water-insoluble dye indicates the presence of micelles and has been used extensively to track this phenomenon since the 1960s.³³ Figures 2 and 3 present the plots of Orange OT and Sudan III dye absorbance values as a function of concentration for **7** and **6**, respectively. UV-vis measurements were conducted to monitor the absorbance of each dye as a function of surfactant concentration in the aqueous samples. After a certain concentration was reached for each surfactant system, the recorded values for each dye at their absorbance wavelength maximums ($\lambda_{\max,OT} = 511$ nm, $\lambda_{\max,SIII} = 523$ nm) are observed to increase with increasing surfactant concentration. This increase in dye absorbance above a specific surfactant concentration indicates the presence of micelles and is attributed to increased dye solubilization as the number of micelles increases.³³ The cmc is obtained by determining the intersection of the slope of this line with the onset of dye absorption for each system. The amount of dye solubilized by the micelles present can be expressed as

$$S = b/(\epsilon L) \quad (1)$$

where S is the amount of dye solubilized, b is the slope of the line fitted to the linear region of the data in Figures 2 and 3, ϵ is the extinction coefficient of the dye (17 400 L/mol·cm for Orange OT and 28 766 L/mol·cm for Sudan 3), and L is the path length (1 cm). The values obtained for dye solubilization in each surfactant system are in general agreement with each other and are presented in Table 1. The solubilizing power of both surfactants appears relatively equal for each respective dye after the cmc has been reached, which is expected since they possess identical hydrophobic segments and differ only by headgroup character.

Figures 2 and 3 also show the responses of dynamic surface tension (operated in equilibrium mode) as a function of concentration for anionic salts **7** and **6** in aqueous solution. The physicochemical properties of a surfactant change to a significant degree after reaching the cmc due to the presence of the micelles and a surfactant saturated air-water interface.³⁴ The surface excess

(33) (a) Schott, H. J. *Phys. Chem.* **1966**, *70*, 2966–2973. (b) Schott, H. J. *Phys. Chem.* **1967**, *71*, 3611–3617.

(34) Lange, R. K. *Surfactants: A Practical Handbook*; Hanser-Gardner: Cincinnati, OH, 1999; pp 13–25.

Table 1. Physicochemical Properties of Surfactants 6 and 7

	cmc ^a (mM)	cmc ^b (mM)	cmc ^c (mM)	Γ (mol/cm ²)	a_{HG} (Å ²)	$\Delta G_{\text{mic}}^{\circ}$ (kJ/mol)	S_{OT}	S_{SIII}
6	2.5	0.6	0.7	4.8×10^{-10}	34.6	-24.8	1.32×10^{-2}	1.89×10^{-3}
7	9.3	2.7	1.4	2.9×10^{-10}	57.1	-21.5	1.00×10^{-2}	1.92×10^{-3}

^a As determined by surface tensiometry. ^b As determined by Orange OT dye solubilization. ^c As determined by Sudan III dye solubilization.

concentration (Γ) and the area per molecule at the interface (a) have been determined using the standard Gibbs equation for anionic surfactants with a swamping amount of electrolyte, which in this case is due to the excess KOH added to solubilize the surfactants, expressed as³⁵

$$\Gamma = -\frac{1}{2.3RT} \left(\frac{d\gamma}{d \log C} \right)_T \quad (2)$$

and

$$a = \frac{10^{16}}{N_{\text{A}}\Gamma} \quad (3)$$

where R is the gas constant, T the temperature at which the measurements were made (26 ± 0.2 °C), γ the surface tension, C the surfactant concentration, and N_{A} Avogadro's number.

A comprehensive listing of all the physicochemical properties calculated for these surfactants is given in Table 1. Each surfactant exhibits the classical dependence of surface tension as a function of concentration, with a constant high surface tension region at low concentrations followed by a decreasing linear region over a concentration range, followed again by a relatively constant region at higher concentrations. Qualitatively, the slope of the linear region for **6** is much steeper than that for **7**, indicating that the phenolate-based anionic surfactant (**6**) assembles at the liquid-gas (L/G) interface with tighter packing when compared to **7**. This is observed quantitatively when comparing the calculated surface excess concentrations of each, which are 2.9×10^{-10} mol/cm² for **7** and 4.8×10^{-10} mol/cm² for **6**. This indicates that **7** has a lower saturation level of free surfactant present at the L/G interface and implies that **7** forms a less tightly packed surfactant layer. The corresponding areas per surfactant molecule at the L/G interface calculated also indicate that carboxylate salt (**7**) occupies a larger area per surfactant molecule (57.1 Å²) than the phenolate salt (**6**) (34.6 Å²). In general, the area occupied by the surfactant molecule at the L/G interface is driven by the area of the *hydrated* hydrophilic portion of the surfactant and not by any one structural element in the molecule.³⁵ Carboxylate anion (**7**) is expected to have a higher degree of hydration relative to phenolate anion (**6**). Furthermore, **6** likely experiences increased electrostatic shielding due to excess potassium ions present in solution which also contributes to **6**'s increased hydrophobicity relative to **7**.³⁵ These combined factors reduce both the degree of hydration and the interfacial area that the phenolate headgroup occupies at the L/G interface.

The S-curves in Figures 2 and 3 also possess two extrapolation points that occur before and after the negative slope region. The concentration at which this latter extrapolation point occurs determines the cmc. The cmc of each surfactant was calculated with this technique by using a least-squares fit of the linear region of the surface tension data and determining the intersection of that line with the constant surface tension values obtained

at higher concentrations. The cmc's calculated from the surface tension data of **7** and **6** are 9.3 and 2.5 mM, respectively. This difference in cmc is again attributed to differences in the electrostatic nature of the anionic headgroups coupled with the great excess of K⁺ ions that are present in solutions of **6** when compared to equimolar solutions of **7**.³⁴ This excess electrolyte screens the electrostatic repulsions between the phenolate headgroups, thereby rendering the surfactant more hydrophobic than its carboxylate counterpart, resulting in a lower cmc value for **6**.³⁵ Overall, the cmc's determined through this method are higher than those obtained by the measurement of dye solubilization described above, as shown in Table 1. This discrepancy is generally attributed to static (dye solubilization) versus dynamic (surface tension) measurements of the microenvironment.³⁶ From the perspective of surface tension values at concentrations greater than the cmc, **6** attains a lower surface tension and thus appears to be a more active surfactant at the L/G interface than **7**.

Surfactants **6** and **7** form micelles at relatively low concentrations, and the standard free energy of micellization ($\Delta G_{\text{m}}^{\circ}$) was therefore determined by using the equation

$$\Delta G_{\text{mic}}^{\circ} = RT \ln \frac{\text{cmc}}{w} \quad (4)$$

where w is the molar concentration of water under ambient conditions (Table 1). The energetically favorable micellization of both surfactants produces negative values for their respective free energies, with -24.8 kJ/mol for **6** and -21.5 kJ/mol for **7**.

To determine the stability of these surfactants in solution, a room temperature aging study was conducted for each. The results, shown in Figure 4, indicate that the surface tension values remain relatively constant for both surfactants over an extended time period (580 h) and do not suffer significant degradation. It should be noted, however, that a slight increase in solution turbidity did occur after 120 h for **7** and 168 h for **6**. This turbidity did not appear to affect the surface tension measurements but may indicate the partial degradation of the surfactant under these storage conditions.

C. Small-Angle Neutron Scattering. The SANS data for 15 mM solutions of each surfactant dissolved in D₂O, and the fitted lines representing model results, are given in Figure 5. The fitted lines, produced by using a polydisperse hard sphere model for **6** and a power-law plus polydisperse hard sphere model for **7**, are in good agreement with the data. The volume fractions produced by both models (0.5%) agree with that determined by the actual surfactant concentration in solution. All of the model results and relevant terms are compiled in Table 2.

The SANS data for **6** exhibit the classical scattering profile associated with spherical micelles. The polydisperse hard sphere model fits the data very well and yields micelles with an average radius of 18.8 Å and a polydispersity of 0.12. The SANS data for **7** appear to have two

(35) Rosen, M. J. *Surfactants and Interfacial Phenomena*, 2nd ed.; Wiley-Interscience: New York, 1989; pp 65–68, 81–83, and 110–117.

(36) Damas, C.; Naejus, R.; Coudert, R.; Frochot, C.; Brembilla, A.; Viriot, M.-L. *J. Phys. Chem. B* **1998**, *102*, 10917–10924.

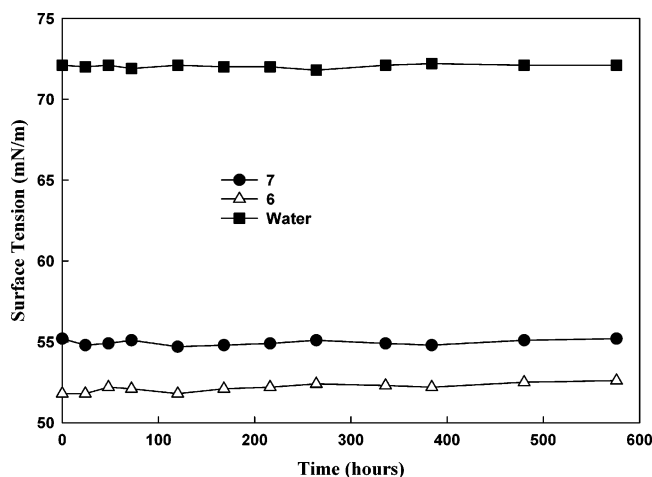


Figure 4. Dynamic surface tension measurements (operated in equilibrium mode) as a function of time at 26 °C for anionic surfactants **6** and **7**, with the surface tension of water measured as a point of reference. The surfactant concentration is 15 mM for both surfactants.

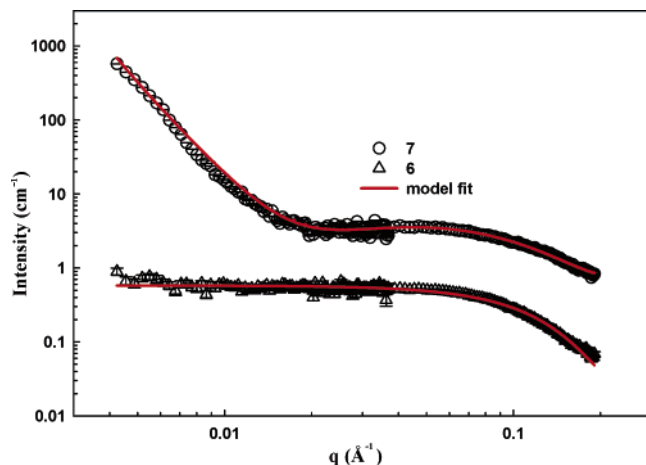


Figure 5. Small-angle neutron scattering data for anionic surfactants **6** and **7**, with model fits of the data presented as solid gray lines for each data set. Models used: polydisperse hard spheres for **6** and power-law plus polydisperse hard spheres for **7**. Note that the data obtained for **7** have been multiplied by a factor of 10 in order to off-set the two curves.

Table 2. Micelle Dimensions Obtained from SANS Data

	r (Å)	polydispersity	volume fraction
6 ^a	18.81 ± 0.002	$0.12 \pm 7 \times 10^{-6}$	$0.0048 \pm 1 \times 10^{-5}$
7 ^b	16.47 ± 0.02	$0.12 \pm 5 \times 10^{-5}$	$0.0041 \pm 2 \times 10^{-5}$

^a Polydisperse hard sphere model results. ^b Power-law plus polydisperse hard sphere model results.

distinct length scales that contribute to the neutron scattering profile, one consisting of micelles that contribute to the scattering data at midrange q values and another consisting of larger-sized structures that create the observed scattering at low q values. This observation led us to fit the data with a model of a power law plus a single population of polydisperse hard spheres, and the model results are in good agreement with the data (Figure 5). The micelle radius 16.5 Å obtained with the polydisperse hard sphere model is consistent with typical spherical micelles and fits the mid and high q ranges of the data from carboxylate (**7**) very well. The power-law exponent obtained from the model (-3.92 ± 0.01) over the lower q range of the data is close to -4 . This value of the slope over the lower q range is consistent with scattering caused by large droplets, aggregates, or precipitates of hydro-

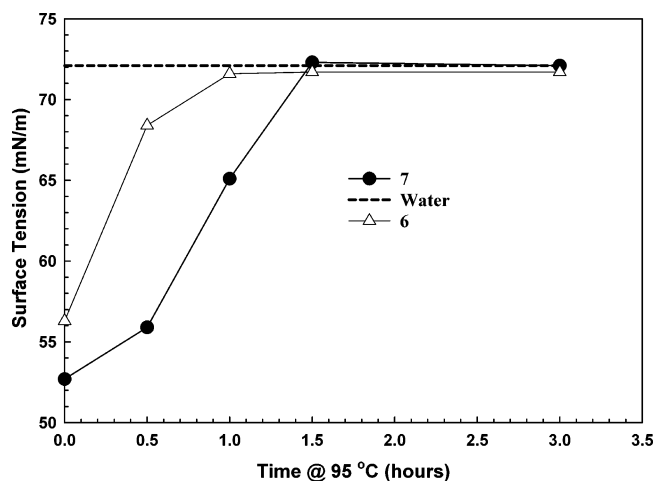


Figure 6. Changes in dynamic surface tension (operated in equilibrium mode) for 20 mM aqueous solutions of anionic surfactants **6** and **7** as a function of time when exposed to 95 °C. Measurements were made at 26 °C. The dashed line represents the surface tension value of water at 25 °C (72.1 mN/m).

phobic material. We therefore attribute this lower q range scattering of **7** to the presence of hydrophobic impurities, aggregates, or partially degraded surfactant. The length scale of this structure is too large to be resolved with SANS. Further investigation into this phenomenon will be conducted in future experiments in order to elucidate the exact structure and composition of these larger-sized structures found in solutions of **7**.

Using the radii obtained from the models and the approximate molecular volumes³⁷ for the phenolate and carboxylate forms, we can calculate the approximate aggregation numbers for the micelles present. This calculation yields aggregation numbers of 39 and 25 for the phenolate and carboxylate micelles, respectively. These values should be considered as a lower bound of the aggregation numbers for these micelles, since the degree of hydration for each surfactant headgroup is unknown. The lower aggregation number calculated for **7** reinforces that these deprotonated surfactant molecules have increased electrostatic repulsions between headgroups when compared to **6**.

D. Surface Tension and Surfactant Response to Temperature. The effect of elevated temperature (95 °C) on 20 mM surfactant solutions of **6** and **7** and the corresponding change in surface tension due to the retro DA reaction were determined by dynamic surface tensiometry. When exposed to elevated temperatures (95 °C), the solutions are observed to undergo a marked color change from clear and colorless to dark yellow and opaque with increased turbidity. Samples were also observed to phase separate when allowed to stand overnight after exposure to this temperature. The responses of the surface tension for 20 mM solutions of **6** and **7** were recorded as a function of time exposed to a temperature of 95 °C, and the data are summarized in Figure 6. Both surfactants are observed to undergo an irreversible loss of surface tension after exposure to this temperature, indicating that the DA fragmentation has occurred. The surface tension value for **7** reaches the value of water (72.1 mN/m) in ~1 h and then stabilizes, whereas it takes 1.5 h for **6** to reach the same plateau range. This difference is ascribed to the different cmc's for each surfactant, as one must

(37) See the Supporting Information for the calculated molecular volumes and aggregation numbers of each surfactant.

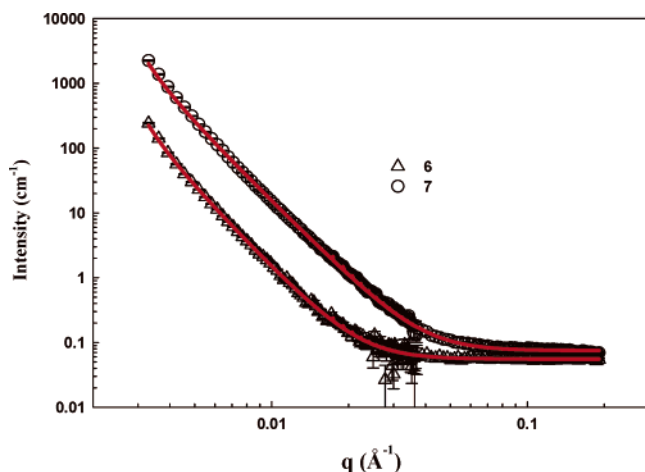


Figure 7. SANS data profiles for the thermally treated aqueous solutions of anionic surfactants **6** and **7** after being exposed for 2 h to a temperature of 95 °C and then cooled to 25 °C. The solid gray lines are fits of the data to a power-law model, which indicate a loss of all micellar structure. The fitted power-law exponents are -4.21 ± 0.01 and -3.96 ± 0.003 for surfactants **6** and **7**, respectively.

reach a lower concentration for **6** before observing a substantial loss of surface tension when compared to **7**, which has a higher cmc. In other words, for the same rate of dissociation, it should require more time for the surface tension measurements of **6** to be affected by surfactant dissociation compared to **7** when starting at identical concentrations. It should also be noted that the measurements of surface tension were taken after the samples had cooled and are convincing evidence that the dissociation accompanying the retro DA is irreversible in micelles.

Surface tension measurements were also conducted on solutions of precursor molecules **1**, **2**, and **3** to determine if these species exhibited any surface-active behavior. Solutions of precursors **1**, **2**, and **3** were prepared and measured in an analogous fashion to surfactant solutions **6** and **7**. Surface tension measurements yielded values of 71.8 ± 0.3 , 72.2 ± 0.2 , and 71.6 ± 0.4 mN/m for molecules **1**, **2**, and **3**, respectively. These results demonstrate that the generation of alkyl furan (**3**) and maleimide potassium salts of **1** and **2** during thermal cleavage of **6** and **7** is expected to produce solutions with surface tension values near those of water (72.1 mN/m at 25 °C).

SANS measurements were also taken to investigate the degradation of micellar structure as a function of temperature and are represented in Figure 7. After exposure to a temperature of 95 °C for 2 h, the scattering profiles for each are markedly different from those presented in Figure 4 and exhibit a lack of the coherent scattering features typically observed for micelles. A change in color and turbidity is also observed macroscopically after this thermal treatment. The scattering that is present in Figure 7 is attributed to large droplets or particles comprised of the hydrophobic fragments of the thermally degraded surfactants. The data are fit well with a power-law plus incoherent background. The fitted power-law exponents obtained are -4.21 ± 0.01 and -3.96 ± 0.003 for surfactants **6** and **7**, respectively, and are close to a slope that corresponds to a q^{-4} dependence that is indicative of structures larger than a few thousand angstroms. The presence of these large-scale structures is also consistent with the visual increase in solution turbidity. The lack of any micellar scattering at higher

q values indicates that there is a complete and irreversible breakdown of all coherent micellar structure after exposure to a temperature of 95 °C for 2 h, which is in agreement with the surface tension measurements presented above.

Conclusions

We have prepared two new surfactants that possess a Diels–Alder adduct integrated into their structures between the hydrophilic and hydrophobic segments that enables the facile thermally induced cleavage of the surfactants into pieces that are unable to form micelles. These surfactants should prove useful as removable templates for the construction of microporous zeolitic materials and for the self-assembly of complex hierarchical materials. The surfactants are soluble in water when their respective phenolic and carboxylic acid salts are formed through headgroup deprotonation by the addition of excess potassium hydroxide. The critical micelle concentrations for the surfactants have been determined through dynamic surface tension measurements and by monitoring the solubilization of water-insoluble dyes in the micellar hydrophobic cores. Small-angle neutron scattering measurements of the aqueous solutions indicate the presence of spherical micelles with radii of 16.5 Å for the anionic carboxylate salt (**7**) and 18.8 Å for the anionic phenolate salt (**6**). The SANS data for carboxylate surfactant (**7**) indicate the presence of another structure at low q that is likely due to small amounts of impurities or micellar aggregates. When the surfactants are exposed to elevated temperatures of 95 °C, the Diels–Alder adduct dissociates, resulting in distinct hydrophilic and hydrophobic fragments incapable of reforming micellar structures. Aqueous solutions of each surfactant subsequently exhibit a loss of all surface-active behavior, and micellar aggregates are no longer detectable through SANS. Phase separation is evident for all thermally treated solutions. There is no observed reversibility of this process when the temperature is lowered to ambient conditions for aqueous solutions of **6** and **7**.

Acknowledgment. The authors thank S. Carmody for large-scale preparation of surfactant molecules and precursors and M. Sprague for additional dynamic surface tension measurements. This work was supported by the United States Department of Energy (US DOE) under contract DE-AC04-94AL85000. Sandia is a multiprogram laboratory operated by Sandia Corporation, a Lockheed Martin Company, for the US DOE. This work was supported in part by the National Science Foundation under Agreement No. DMR-9986442. Los Alamos National Laboratory, an affirmative action/equal opportunity employer, is operated by the University of California for the United States Department of Energy under contract W-7405-ENG-36. Certain trade names and company products are identified in order to specify experimental procedures adequately. In no case does such identification imply recommendation or endorsement by the National Institute of Standards and Technology, nor does it imply that the products are necessarily the best available for the purpose.

Supporting Information Available: Aggregation number calculations and ^1H and ^{13}C NMR characterization data. This material is available free of charge via the Internet at <http://pubs.acs.org>.

LA047074Z